The International Journal of Analytical and Experimental Modal Analysis v 7 n 4 p 243-253 Oct 1992

[redacted]

by P. Q. Zhang, University of Wisconsin-Madison; Q. M. Wang and X. P. Wu, University of Science and Technology of China; T. C. Huang, University of Wisconsin-Madison

ABSTRACT

In this paper, we analyze theoretically the use of correlation statistical properties in the random speckle field, in the non-contact recording of free-response information of vibrating objects, and in terms of time-domain signals collected simultaneously at multiple points, and we use system identification techniques in the frequency and time domains to identify the dynamic parameters. The bending vibration of a miniature cantilever beam and the torsional vibration of a miniature shaft with 3-degrees of freedom are measured. The dynamic property parameters identified are in good agreement with the theoretical values. By the same process, the lower-order natural frequencies and modes of the bending arm of a dental drill are measured and analyzed.

1. Introduction

The dynamic property analysis of precision mechanisms, computer reading and writing heads, central parts of a watch, miniature vibration and pressure sensors, components of large-scale integrated circuits, miniature bellows, etc. are of vital importance to the dynamic design for vibration isolation and for quality improvement of such products. In recent decades, experimental modal analysis using interdisciplinary analytical techniques has developed rapidly with the advance of computer and measurement technology. Because of the small weight of miniature structures (several grams to several tens of grams) and of the tiny areas available for the installation of a sensor (the diameter being below several millimeters), it is difficult to install the sensor without the mass and the rigidity of the sensor changing the dynamic properties of the original structure. Non-contact measurement devices such as the electrical eddy current sensors are only suitable for the measurement of ferro-magnetic substances; moreover, the diameter is at least several millimeters. Traditional optical measurement techniques, such as time-averaged holography, random speckle line patterning, and the stroboscope, require that the object's vibration be steady. This causes loss of time information and, therefore, limits their application. For the various reasons above, the analysis and research of the dynamic properties of miniature objects has aroused the interest of scientists.

In this paper, we analyze theoretically the use of the correlational statistical properties of a random

---

P. Q. Zhang, Visiting Scholar, Dept. of Engineering Mechanics, University of Wisconsin-Madison, Madison, WI 53706 and Associate Professor, Department of Modern Mechanics of the University of Science and Technology of China (USTC). Q. M. Wang, Lecturer, Department of Precision Machinery, USTC. X. P. Wu, Professor, Department of Modern Mechanics, USTC. T. C. Huang (SEM member), Professor, Department of Engineering Mechanics, University of Wisconsin-Madison, Madison, WI 53706.

Final manuscript received: March 27, 1992

speckle field in the real-time recording of the responses of three miniature structures in the time domain. The time-domain signals are collected simultaneously at multiple points. We conduct system parameter identification techniques by three different approaches (including both frequency-domain and time-domain methods).

The bending vibration of a miniature cantilever beam and the torsional vibration of a small shaft with 3-degrees of freedom are tested. The system parameter identification results of these dynamic properties are in good agreement with their theoretical values. Also, by the same process, the lower-order natural frequencies and the modes of a small dental drill are measured and analyzed. Thus, we can see that the process, with optical measurement and computer analysis, has the advantage of dealing with non-contact measurements, with miniature target areas (diameter below 0.5 mm), with closely space measurements (approximately 1 mm) and with rapid responses at multiple points. Nonstationary time-domain signals are measured simultaneously. This provides an effective way to identify the dynamic parameters of miniature objects without disturbing the object itself.

2. Theoretical Fundamentals

(a) Experimental Principles of Optical Measurement

(1) Arrangement of Experimental Light Paths

Figure 1 shows an object illuminated by a laser beam. This illumination generates a spatially random speckle pattern. Plate H is located at a distance z from the object surface. The plate is a film taken of the random speckle pattern, developed and fixed when it is not vibrating. Thus, the static random speckle pattern of the diffuse reflective object is recorded on the plate. Behind the plate, lens L focuses the light reflected by the object and the light passing through the plate onto the photoelastic multiplier D.

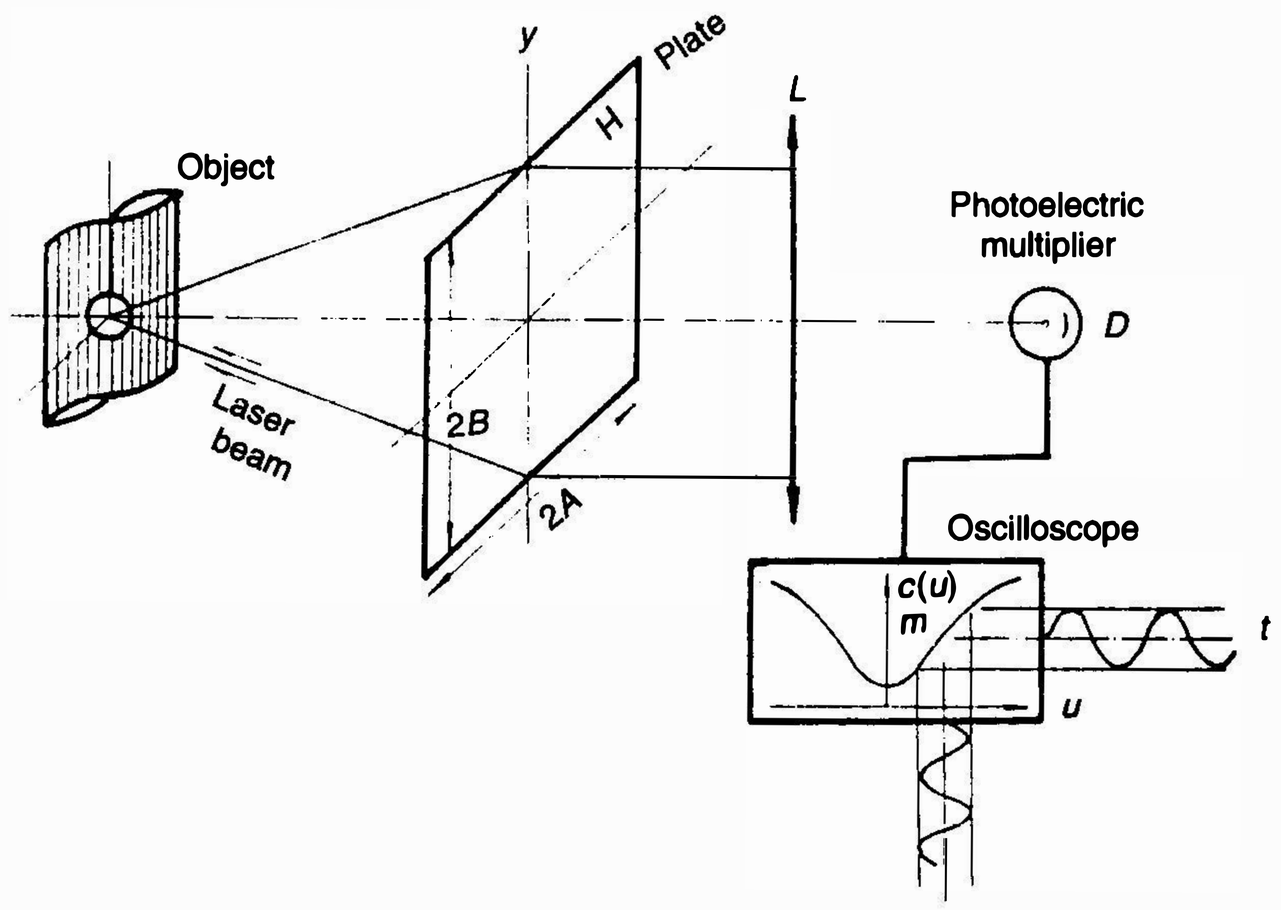

Fig. 1 Principle of optical measurement

(2) Motion Laws of Space and Random Speckle [1]

When the surface of the object deforms, the relationship between its displacement, displacement differentiation and the displacement of the space speckle is determinate. If the motion of the space speckle is measured, then the surface displacement and the spatial derivatives of the surface displacement of the object may be calculated.

As illustrated in Fig. 2, surface component Σ is illuminated from source s, and is observed from spatial p. In Fig. 2 ρ_{so} and ρ_{po} are the illuminating and observing distances respectively, (ℓ_s, m_s, n_s) and (ℓ_p, m_p, n_p) are the direction cosines of $o\vec{s}$ and $o\vec{p}$ respectively. The motion parameters of the surface component are (u, v, w) and $\left(\frac{\partial u}{\partial x}, \frac{\partial u}{\partial y}, \frac{\partial v}{\partial x}, \frac{\partial v}{\partial y}, \frac{\partial w}{\partial x}, \frac{\partial w}{\partial y}\right)$. In the practical measurement, in Fig. 3, when $\ell_p = 0$, we establish the coordinate system $(p - x, \eta, \xi)$, and in this system the speckle displacement formula [1] is

$$\begin{Bmatrix} u_x \\ v_\eta \\ w_\xi \end{Bmatrix} = \left\{ \begin{bmatrix} 1 & 0 & 0 \\ 0 & n_p & -m_p \\ 0 & m_p & n_p \end{bmatrix} + \frac{\rho_{po}}{\rho_{so}} \begin{bmatrix} 1-\ell_s^2 & -\ell_s m_s & -n_s \ell_s \\ -m_s \ell_s / n_p & \left(1-m_s^2\right)/n_p & -m_s n_s / n_p \\ 0 & 0 & 0 \end{bmatrix} + \frac{\rho_{po}^2}{\rho_{so}^2} \begin{bmatrix} 0 & 0 & 0 \\ 0 & 0 & 0 \\ \ell_s & m_s & n_s \end{bmatrix} \right\} \begin{Bmatrix} u \\ v \\ w \end{Bmatrix}$$

$$+\rho_{po} \begin{bmatrix} -\ell_p & 0 & -\left(m_s+m_p\right) & 0 & -\left(n_s+n_p\right) & 0 \\ 0 & -\frac{\ell_s}{n_p} & 0 & -\frac{m_s+m_p}{n_p} & 0 & -\frac{n_s+n_p}{n_p} \\ 1+\frac{\rho_{po}}{\rho_{so}} & 0 & 0 & 1+\frac{\rho_{po}}{\rho_{so}} & 0 & 0 \end{bmatrix} \begin{Bmatrix} \frac{\partial u}{\partial x} \\ \frac{\partial u}{\partial y} \\ \frac{\partial v}{\partial x} \\ \frac{\partial v}{\partial y} \\ \frac{\partial w}{\partial x} \\ \frac{\partial w}{\partial y} \end{Bmatrix} \tag{1}$$

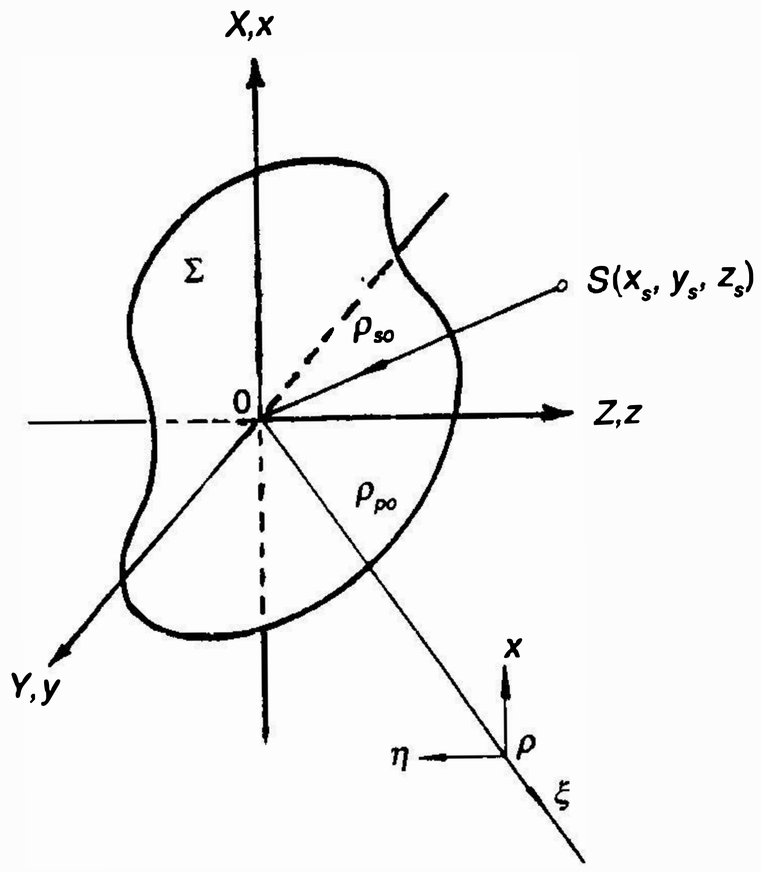

Fig. 2 **Laser beam on a deformed object**

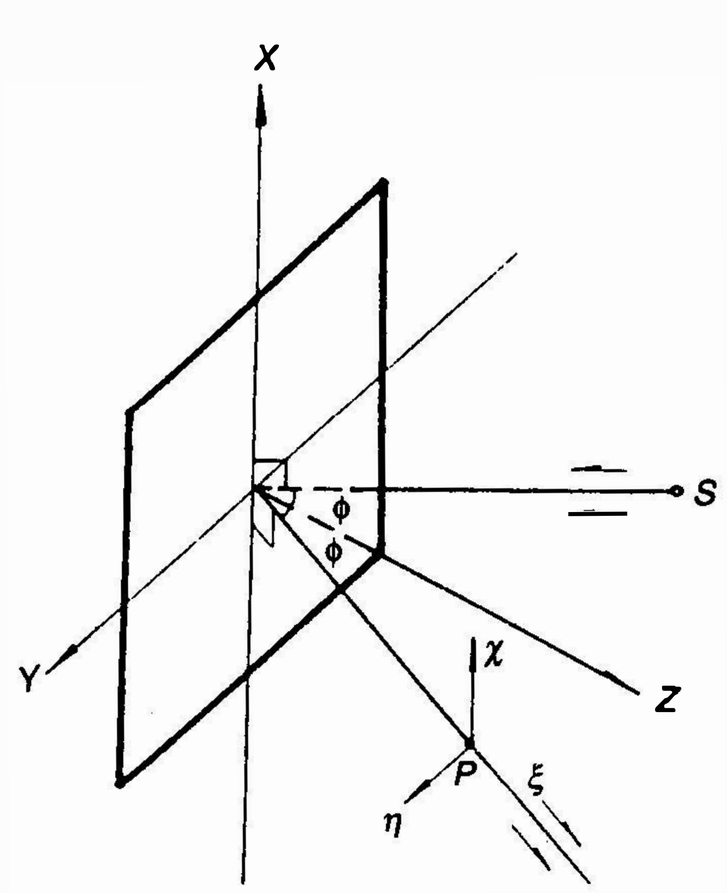

Fig. 3 **A special case of laser beam arrangement**

If the light path is arranged as shown in Fig. 3, $\ell_p = \ell_s = 0$ (the observing and illuminating directions are both in the plane yoz) and $m_p = -m_s$, $n_p = n_s$ (the illuminating and observing directions symmetrical about the z axis), then for

i) One-dimensional in-plane vibration of object $u = u(t)$, the displacement formula of speckle is simplified to

$$u_x = \left(1 + \rho_{po} / \rho_{so}\right) u = \alpha u \tag{1a}$$

where $\alpha = (1 + \rho_{po} / \rho_{so})$ = constant and v_η, $w_x = 0$.

ii) Torsional vibration of the revolving object (twisted around y axis), to assume $\delta\phi_y = \delta\phi_y(t)$, where $\delta\phi_y = -\dfrac{\delta w}{\delta x}$

The displacement formula of speckle can be simplified to

$$u_x = 2\rho_{po} n_s \delta\phi_y + \left[1 + \rho_{po} / \rho_{so}\right] R\delta\phi_y = \gamma\delta\phi_y \tag{1b}$$

where $\gamma = 2\rho_{po} n_s + [1 + \rho_{po} / \rho_{so}]R$ = constant, and where R is the radius of rotation, then $u_x(t) = \gamma\delta\phi_y(t)$.

(3) Speckle Intensity Received by the Photoelectric Multiplier

Let the intensity of the random speckle field on plate H be $I(x,y)$, and the intensity transmittance of the plate after exposure and processing be $T = 1 - \beta I(x,y)$, where β is a constant. The plate is negative film. When the object is static, the light speckle in the random speckle field fits with the dark speckle on the plate. At this moment, the laser lights passing through the plate have the least intensity when they are received by the photoelectric multiplier. When the object has small displacement (u,v), translation along x and y axes, the structure of the random speckle field has no variation except for an overall translation on plane H.

Thus, the light intensity received by the photoelectrical multiplier is proportional to the correlation function $C(u_x, v_\eta)$. There $C(u_x, v_\eta)$ is

$$C\left(u_x, v_\eta\right) = \frac{1}{4AB} \int_{-B}^{B} \int_{-A}^{A} \left\{ I\left(x + u_x, y + v_\eta\right)\left[1 - \beta I(x,y)\right] \right\} dxdy \tag{2}$$

where A, B are the half-height and half-width of the plate, respectively. For simplicity, we only consider the translation u of the object along x axis. Its functional curve is illustrated in Fig. 1

When the object is static, we can offset the plate by a suitable displacement along the x axis to cause the light intensity on the photoelectric multiplier to be located at the center m of the linear area of the correlation function like light intensity. Thus, as long as the translation u_x of the random speckle field is controlled below half of the speckle size, the light intensity $C(u_x)$ received by the photoelectric multiplier will vary in the linear range.

When the object vibrates at the equilibrium position, $u = u(t)$ varies. Let the gradient of the linear segment of $C(u_x)$ be κ. The light intensity at point m is $C(m)$, then the light intensity of the photoelectric multiplier is

$$C(t) = C\left(u_x(t)\right) = C(m) + \kappa u_x(t) = C(m) + \kappa\alpha u(t) \tag{3}$$

as illustrated in Fig. 1. Thus, we can make a real-time tracking of the object movement using function $C(t)$, since the light intensity is the result of the optical correlation process occurring at the plate H.

(b) Computer Analysis-Dynamic Parameter Identification of the System

When the object is struck lightly by a little hammer, the time-transient force-response of the object's vibration can be obtained from the photoelectric transformation described above. The related modal parameters are calculated in terms of the time-domain signals collected simultaneously at multiple points by multiple photoelectric transformers and by means of the time-domain identification techniques presented by the author in 1986, i.e., single-input and multiple single-input space-time regressive methods (S-STRM, MS-STRM) [2]. The derivation is simplified as follows.

According to linear vibration theory, the recursion formula for the free response of a system with N degrees of freedom is given as

$$x_i(k) = \sum_{q=1}^{L} \sum_{j=1}^{N} a_{ij}^{q} x_j(k-q) \qquad i = 1,2,\ldots,N \qquad k = L+1,\ldots,L+m \tag{4}$$

where N is the number of measured points and m is the number of sampled points. The formula denotes that the response of a measured point i at moment k is determined by the L numbers of sampled values before moment k at the N numbers of measured points. a_{ij}^{q} is the space-time regression coefficient. The above sum expression can be written in matrix form

$$\{x(k)\} = \sum_{q=1}^{L} A^{q} \{x(k-q)\} \tag{5}$$

where

$$\{x(k)\} = \begin{Bmatrix} x_1(k) \\ x_2(k) \\ \vdots \\ x_N(k) \end{Bmatrix}_{N\times 1} \qquad A^{q} = \begin{bmatrix} a_{11}^{q} & a_{12}^{q} & \cdots & a_{1N}^{q} \\ a_{21}^{q} & a_{22}^{q} & \cdots & a_{2N} \\ \vdots & \vdots & \cdots & \vdots \\ a_{N1}^{q} & a_{N2}^{q} & \cdots & a_{NN}^{q} \end{bmatrix}_{N\times N} \qquad q = 1,2,\ldots,L$$

The above equation presents the free response of N measured points generated by a single-input at an arbitrary position. By means of the methods of least squares, we can solve the system matrix under the single-input and upon which other operations can be made. This is called the single-input space-time regression method. Let p be the total number of different excitation positions where samples were taken from the output, the equation of multiple single-input space-time regression can be written as

$$\left[\{x^1(k)\},\{x^2(k)\},\ldots,\{x^p(k)\}\right] = -\sum_{q=1}^{p} A^{q}\left[\{x^1(k-q)\},\{x^2(k-q)\},\ldots,\{x^p(k-q)\}\right] \tag{6}$$

From modal theory, we know that

$$\{x(k)\} = \begin{Bmatrix} x_1(k) \\ x_2(k) \\ \vdots \\ x_N(k) \end{Bmatrix} = \begin{bmatrix} \psi_{11} & \psi_{12} & \cdots & \psi_{1N} \\ \psi_{21} & \psi_{22} & \cdots & \psi_{2N} \\ \vdots & \vdots & \cdots & \vdots \\ \psi_{N1} & \psi_{N2} & \cdots & \psi_{NN} \end{bmatrix} \begin{bmatrix} e^{\lambda_1 k\Delta} \\ e^{\lambda_2 k\Delta} \\ \vdots \\ e^{\lambda_N k\Delta} \end{bmatrix} \tag{7}$$

where $\psi = [\psi_{ij}]$, $(i,j = 1,2,\ldots,N)$ and λ_i, $(i = 1,2,\ldots N)$ are the eigenvector matrix of the system matrix (i.e., modal matrix) and the eigenvalue of the system matrix respectively and Δ is the sampling interval. Substituting Eq. (7) in Eq. (6), we have

$$\sum_{q=o}^{L} A^q \psi \begin{Bmatrix} e^{\lambda_1(k-q)\Delta} \\ e^{\lambda_2(k-2)\Delta} \\ \vdots \\ e^{\lambda_N(k-q)\Delta} \end{Bmatrix}_{POE} = 0 \qquad POE = 1,2,\ldots,p \tag{8}$$

where A^0 is unit matrix, A^q $(q = 1,2,\ldots,L)$ is space-time regression coefficient matrix and POE is position of the exciter. From Eq. (6) we solve A^q. Then the system matrix $A^q = [A^0, A^1, \ldots, A^L]$, which contains the information of how multiple input can be obtained, and the system modal parameters are finally determined by solving the eigenproblem [3].

By means of the resolution of a singular value, we can make the solution much more precise and stationary. With an overdetermined mathematical model, we use OAMCF (Overall Modal Confidence Factor) as an efficient method in determining the model order. We use the simple and practical multiple single input to construct a system matrix of multiple input information, which can improve the precision and reduce the experiment cost. Meanwhile, it provides the global identification properties. In order to improve the quality of time-domain signals, we preprocess by low-pass filtering and use multiple averaging on the system matrix elements, both of which give good results.

FDM (Frequency Domain Method) is the monitoring of the amplitude and phase of response under various orders of natural frequencies. An HP 3582 spectrum analyzer was used in obtaining the dynamic parameters, similar to the frequency domain curve fitting method of one degree of freedom.

3. Experiment

(a) Experiment Approach

The complete measurement and analysis system roughly consists of three sections: light-path arrangement, collecting and monitoring vibration signals and computer analysis. The block diagram of the experiment is shown in Fig. 4 and the light-path arrangement is shown in Fig. 5.

(b) Experimental Examples

Example 1: The bending vibration of a miniature cantilever beam is measured. The beam is made of copper ($75 \times 7 \times 1.5$ mm) and the diameter of the laser target is under 0.5 mm. Three different methods are used in the identification of the five lower-order natural frequencies and mode shapes, the results are shown in Fig. 6 and Table 1.

Example 2: The torsional vibration of a small shaft is measured. The shaft has 3-degrees of freedom (three circular plates with diameter = 30 mm, depth =3 mm, and 40 mm distance between the plates). Three different methods are used to identify the three lower-order natural frequencies and mode shapes. The results are shown in Fig. 7 and Table 1.

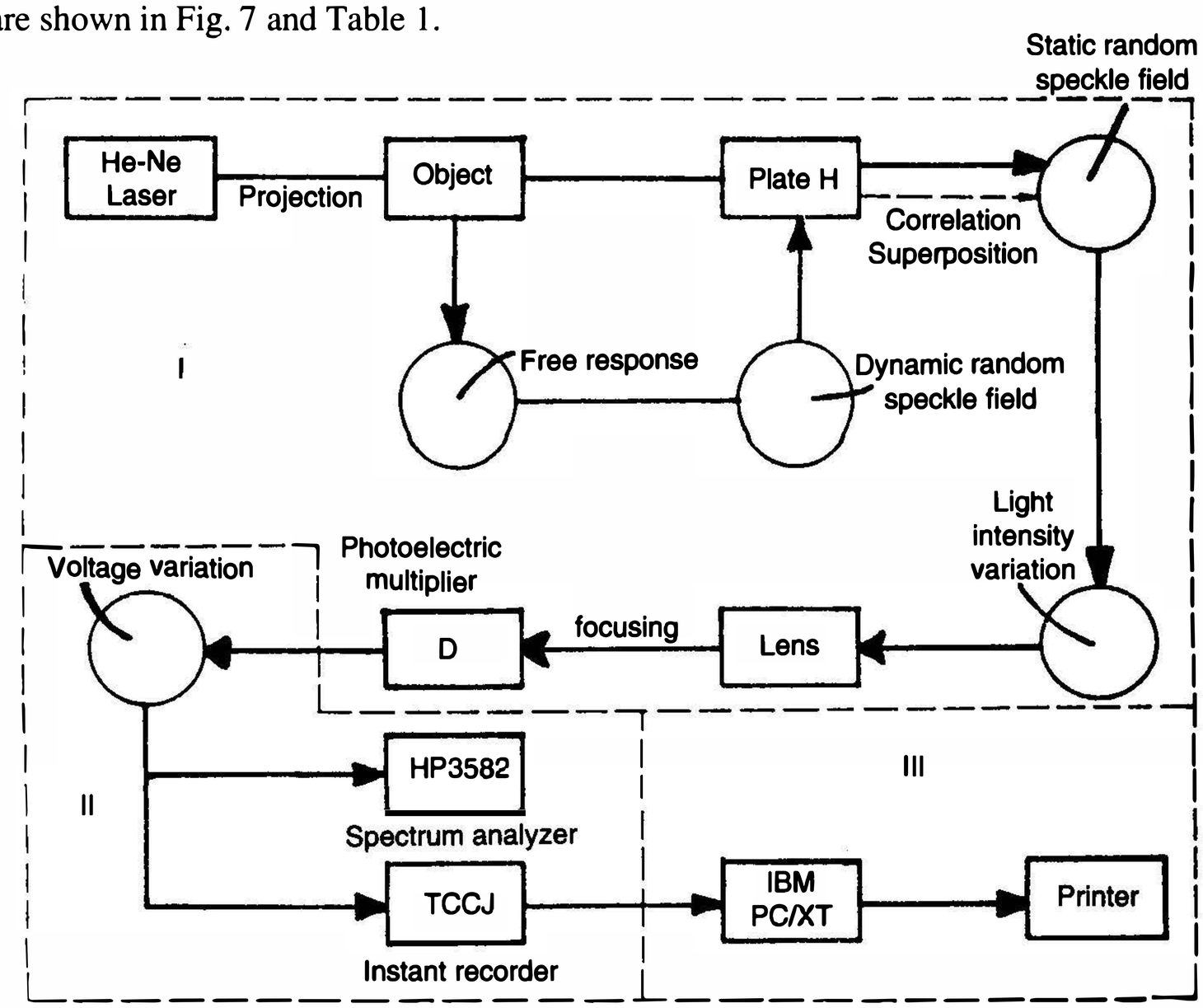

Fig. 4 Block diagram of the experiment: I. laser measurement, II. data acquisition, III. modal analysis

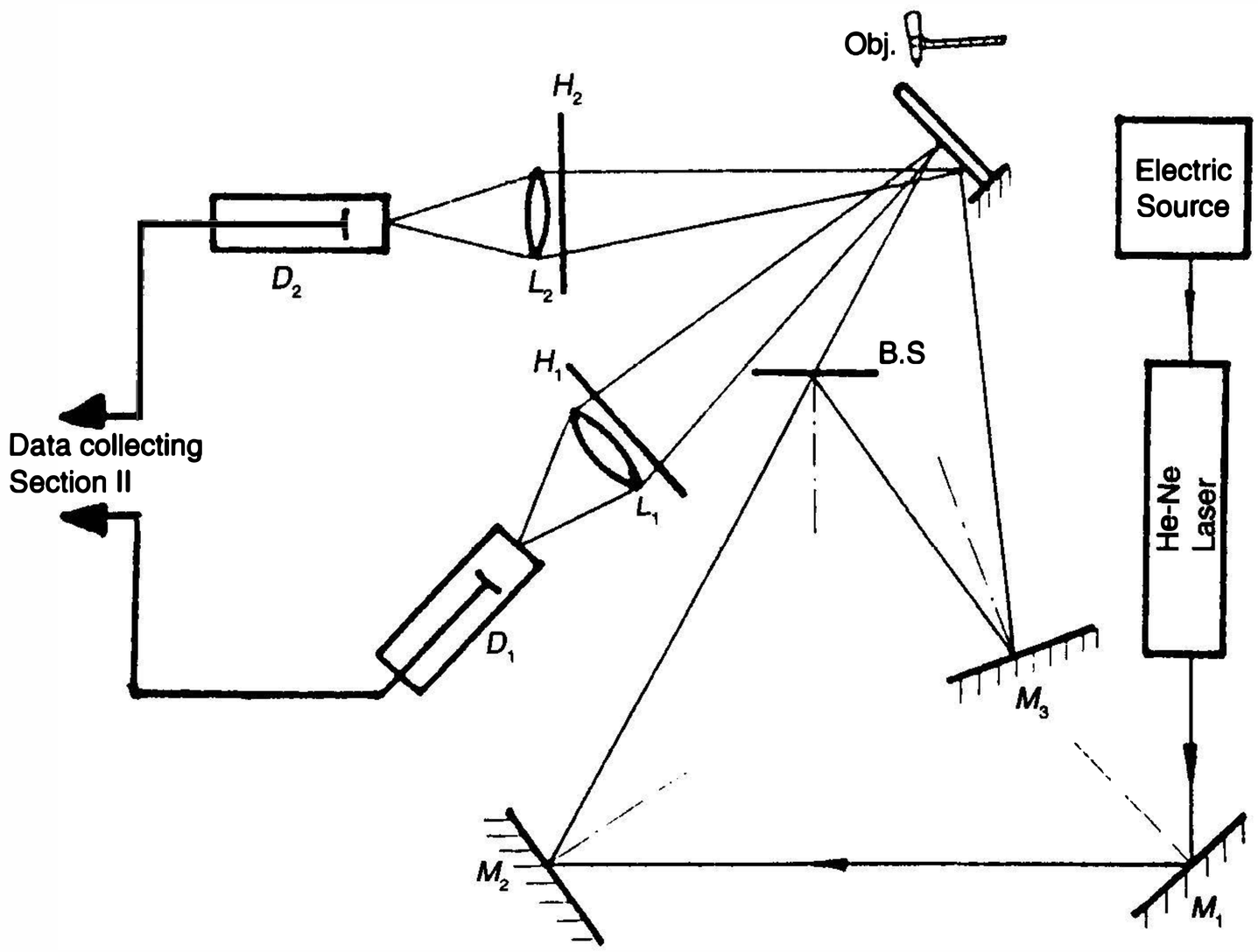

Fig. 5 Light path of the laser measurement

Example 3: Findings from the measurement of the lower-order natural frequencies and modes of the bending arm of a small dental drill with a length of approximately 60 mm are shown in Fig. 8, and Table 1 [4].

TABLE 1 THE NATURAL FREQUENCIES OF THE DENTAL DRILL, THE TORSIONAL SHAFT AND THE CANTILEVER BEAM.

Mode		Frequency (error %) Hz			
		Theory	Identification		
			FDM	S-STRM	MS-STRM
dental drill	1	---	750	---	750
	2	---	825	---	848
	3	---	3200	---	3112
	4	---	---	---	4094
small size shaft with 3 degrees of freedom	1	133	136 (2.3)	134 (0.8)	134 (0.8)
	2	372	376 (1.1)	367 (1.3)	367 (1.3)
	3	532	540 (1.5)	527 (0.9)	528 (0.8)
mini-size cantilever beam	1	140	144 (2.9)	141 (0.7)	141 (0.7)
	2	878	904 (3.0)	863 (1.7)	875 (0.3)
	3	2457	2480 (0.9)	2479 (0.9)	2444 (0.5)
	4	4815	5060 (5.0)	4978 (3.4)	4837 (0.4)
	5	7959	8080 (1.5)	8161 (2.5)	8046 (1.1)

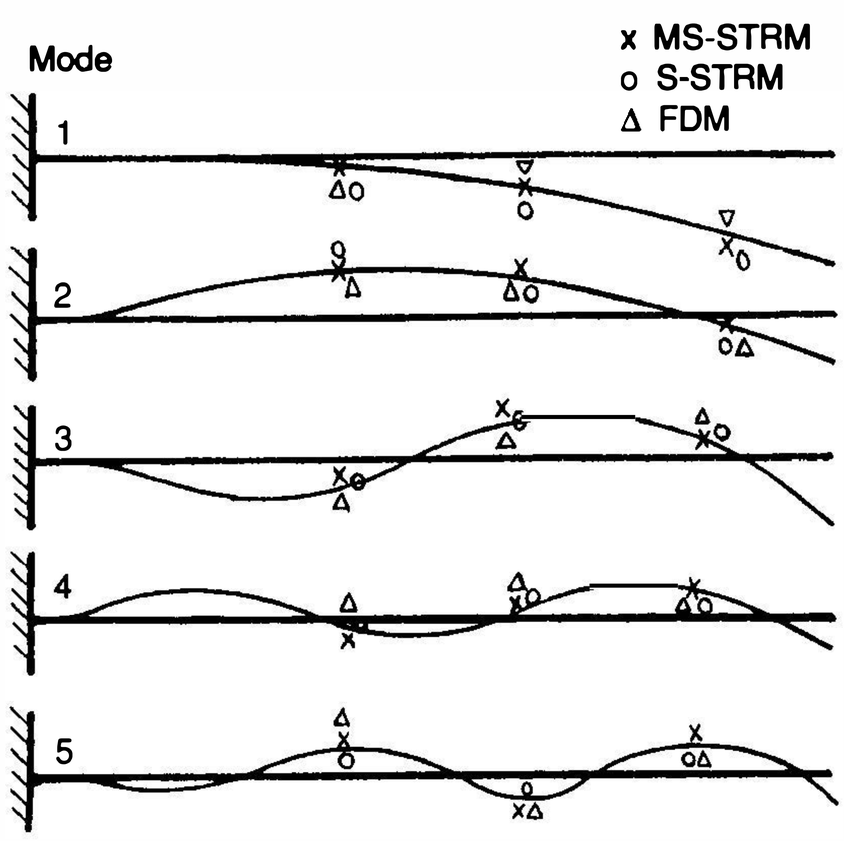

Fig. 6 Mode shapes of a miniature cantilever beam

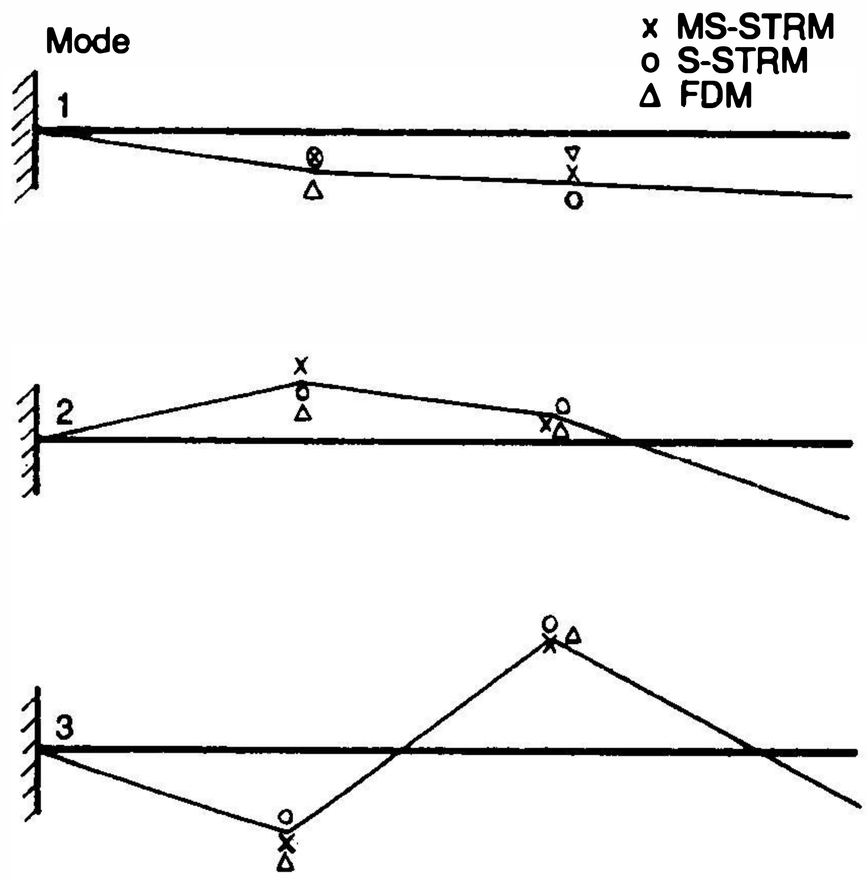

Fig. 7 Mode shapes of a small shaft

(c) Technical Details [5,6]

From the derivation and experiments mentioned above, we can conclude that it is of vital importance to ensure that the transformation from object displacement to light intensity should be linear at the various sectors. For this reason, the following should be ensured in the experiment:

i) The offset of the plate should be in the linear range of the correlation function.

ii) The impact should be moderate. On the one hand, the impact duration should be short to ensure that the input autospectrum has a smooth spectrum of enough width. This impact will excite higher order natural frequencies of the object. On the other hand, the impact should not be too large, otherwise the dynamic and static random speckle fields may not be correlated.

iii) The operation of film developing and film fixing of the plate should be in accordance with the plate properties, thus making the plate transmissivity in the linear range.

iv) Adjust the voltage of the high voltage source of the photoelectric multiplier to ensure the voltage and the light intensity have a linear relationship.

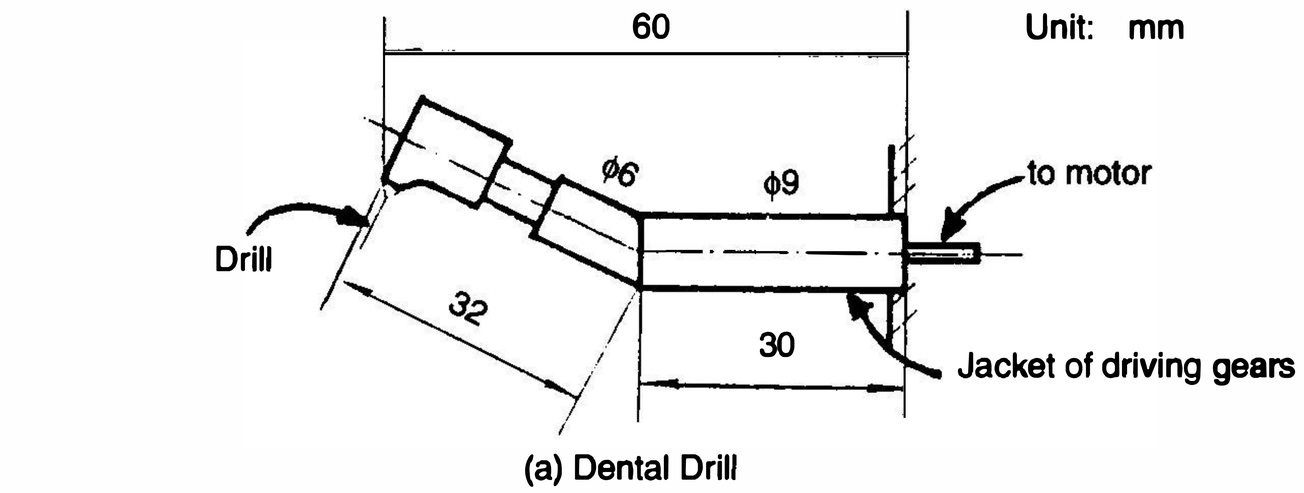

(a) Dental Drill

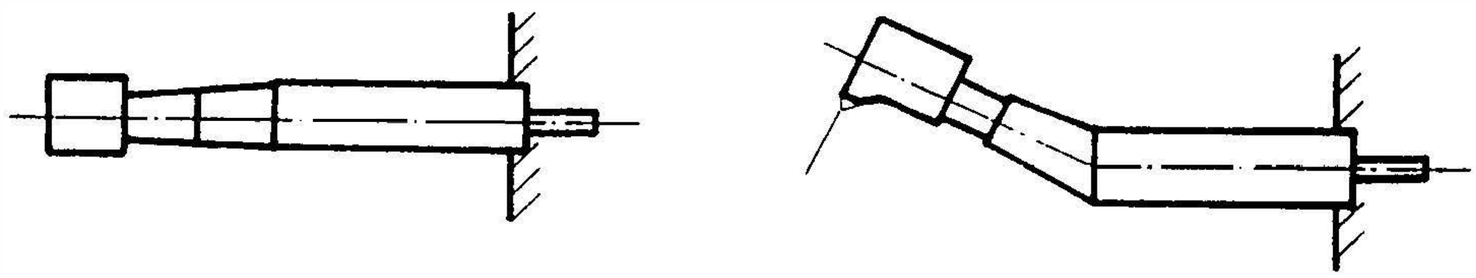

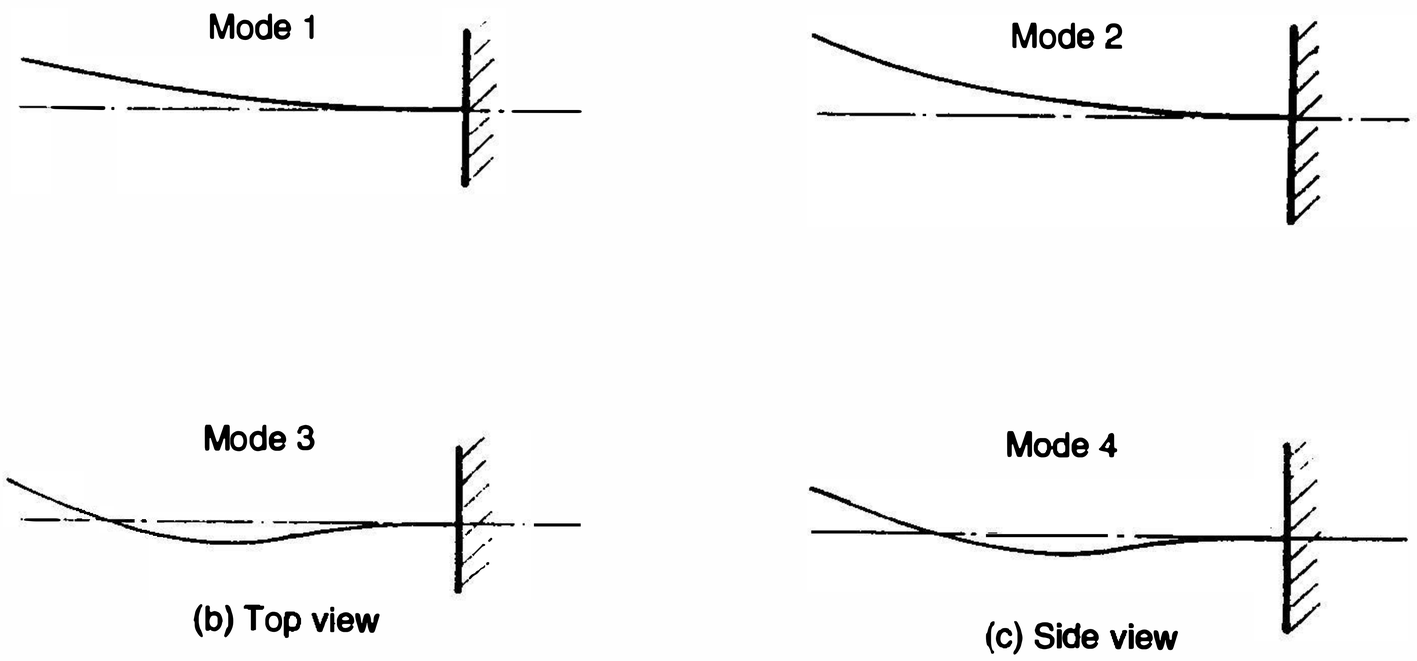

(b) Top view

(c) Side view

Fig. 8 Mode shapes of a dental drillarm

v) Adjust the measurement range and sensitivity to ensure that the random speckle has enough size.

It is known that the size of the random speckle is: $\sigma = 1.2\frac{\lambda z}{D}$ (D is the diameter of the reflective surface component, z is the distance between the illuminated surface and the light source, λ is wave length). By adjusting z and D, we can control the size of σ.

In the measurement of time-domain signals collected simultaneously at multiple points by the output of the photoelectric multipliers, signals of each group (for example, two points measured simultaneously in each group) are normalized and static calibration is used.

4. Results and Discussion

The identification results of the three methods, S-STRM, MS-STRM and FDM are in good agreement with the theoretical calculations. Also the identification precision is satisfactory.

The relative error of the miniature cantilever (first 5 orders) by the three methods does not exceed 3.4%; the relative error of the torsional shaft (first 3 orders) does not exceed 2.3%. The deviations of the phase angle of the torsional shaft are generally below 10° (using the reference of the real mode). The results of miniature cantilevers are less satisfactory. As to the relative error of the amplitude of modal vectors, the torsional shaft is 3-5% and the miniature cantilever is a little more.

Generally speaking, the results of MS-STRM (input three times) are better than that of S-STRM, and FDM ranks third. This is mainly due to the fact that multiple single-inputs constitute a system matrix of multi-input information and has the advantages of a multi-input multi-output system identification procedure especially in the case of close modes, heavy damping and low signal-noise ratio. Also the experimental cost is lower.

When system matrices of the same order are used, the MS-STRM needs the least length of the sampling data. S-STRM is a special case of MS-STRM when $p = 1$. FDM is an equivalent of the one degree of freedom fitting in the frequency domain. Only under separate modes and low damping can the results of FDM be satisfactory.

5. Conclusion

Experiments prove that this combination of optical measurement and computer analysis has the following outstanding advantages: i) non-contact measurement, ii) no applied mass and rigidity, iii) small target area (diameter below 0.5 mm), iv) measurements of small space interval (approximately 1 mm), v) rapid response and vi) obtaining multiple non-stationary time-domain vibration signals in one measurement. Furthermore, the experiment is stable and highly precise. The process will be an efficient tool in the research of the dynamic properties of miniature objects.

Acknowledgment

This project has been supported in part by the Natural Science Foundation of China.

References

1. Wu, X.P.; He, S.P.; Li, Z.C. "Motion laws of space random speckle." *Physics Journal* v 29 n 9 Sept 1980.
2. Huang, T.C.; Zhang, P.Q.; Feng, W.Q. "Multiple single-input space-time regression method in modal analysis." *Int J Anal Exp Modal Anal* v 1 n 4 p 1-7 Oct 1986.
3. Recklin, G.T "The numerical implementation of a multi-input estimation method for mini-computer." *Proceedings of the 1st International Modal Analysis Conference*, Orlanda, FL, Nov. 8-10, 1982. p 542-548
4. Zhang, P.Q.; Wang, Q.M.; Tang, X.O.; Huang, T.C. "Modal analysis of mini-small object--dental drill." In: Huang, T.C. (ed.) *Modal Analysis, Modeling, Diagnostics, and Control: Analytical and Experimental.* New York: American Society of Mechanical Engineers; 1991. v DE-38 p 17-23
5. Zhang, Q.C. *Analytical Techniques and its Application of the Dynamic Laser Speckle Spectrum.* M.S. Thesis, University of Science and Technology of China, 1987.
6. Tang, X.O. *Parameter Identification of Mini-small Object.* B.S. Thesis, University of Science and Technology of China, 1990.

SEM Fall Conference

Sheraton Chicago Hotel
Chicago, Illinois

November 16-20, 1993

Joint Conference with the American Society for Nondestructive Testing

For additional information contact: Society for Experimental Mechanics, Inc., 7 School Street, Bethel, CT 06801

DINAME 93
Symposium on Dynamic Problems of Mechanics

Hotel Plaza Caldas da Imperatriz
Santo Amaro, Santa Catarina, Brazil

March 1-5, 1993

Sponsored by: Brazilian Society for Mechanical Sciences

For additional information contact: Eduardo M.O. Lopes, Laboratório de Vibrações e Acústica, Departamento de Engenharia Mecânica, C.P. 476, Florianópolis, SC, Brazil, CEP 88049

STRUCTRURAL DYNAMICS MODELING
Test, Analysis and Correlation

Cranfield, U.K.

July 7-9, 1993

Co-Sponsored by: Dynamic Testing Agency (DTA) and National Agency for Finite Element Methods and Standards (NAFEMS)

For additional information contact: Mr. Neil Harwood, DTA Conference Office, NEL, East Kilbride, Glasgow G75 0QU, U.K. Phone: 44/0 3552-72363 Fax: 44/0 3552-72047